

# Highly Viscoelastic Wormlike Micellar Solutions Formed by Cationic Surfactants with Long Unsaturated Tails

Srinivasa R. Raghavan and Eric W. Kaler\*

Center for Molecular and Engineering Thermodynamics, Department of Chemical Engineering, University of Delaware, Newark, Delaware 19716

Received June 5, 2000. In Final Form: August 9, 2000

Cationic surfactants having long ( $C_{22}$ ) mono-unsaturated tails were studied in aqueous solutions containing salt using steady and dynamic rheology. The surfactant erucyl bis(hydroxyethyl)methylammonium chloride self-assembles into giant wormlike micelles, giving rise to unusually strong viscoelasticity. Under ambient conditions, the viscosity enhancement due to surfactant exceeds a factor of  $10^7$ . Some samples behave as gel-like solids at low temperatures and revert to the viscoelastic (Maxwellian) response only at higher temperatures. These samples display appreciable viscosities ( $> 10$  Pa·s) up to very high temperatures (ca.  $90$  °C). Salts with counterions that penetrate into the hydrophobic interior of the micelles, such as sodium salicylate, are much more efficient at promoting self-assembly than salts with nonbinding counterions, such as sodium chloride. Changing the surfactant headgroup to the more conventional trimethylammonium group reduces the viscosity at high temperatures.

## Introduction

Cationic surfactants can self-assemble into long, flexible wormlike micelles in the presence of salt, and the entanglement of these micelles into a transient network imparts viscoelastic properties to the solution.<sup>1,2</sup> These micelles can thus function as thickening and rheology-control agents in aqueous systems, much like polymers. This provides a practical illustration of the analogy between wormlike micelles and polymers.<sup>3–6</sup> Unlike polymers, however, wormlike micelles are in thermal equilibrium with their monomers. Thus, micellar self-assembly (and hence, their length and flexibility) responds to changes in surfactant and salt concentration, nature of counterion, and temperature.

Theory and experiments suggest that the micellar contour length  $\bar{L}$  decays exponentially with increasing temperature.<sup>5,6</sup> Concomitantly, key rheological parameters such as the zero-shear viscosity  $\eta_0$  and the relaxation time  $t_R$  also decrease exponentially. An Arrhenius plot of  $\ln \eta_0$  versus  $1/T$  (where  $T$  is the absolute temperature) is a straight line, the slope of which yields the activation energy  $E_a$ .<sup>7</sup> A wide range of  $E_a$  values ( $70$ – $300$  kJ/mol) are reported for various micellar systems.<sup>7–16</sup> The systematic variation

in rheology with temperature also facilitates rheological master curves through time–temperature superposition.<sup>9–12</sup>

Temperature effects on wormlike micellar solutions in the semidilute regime have been studied mainly for surfactants with a saturated hydrocarbon tail of  $C_{16}$  or shorter.<sup>7–16</sup> In particular, cetyl trimethylammonium halides ( $C_{16}$ TAX) and their analogues with hydrophobic counterions such as salicylate, tosylate, or dichlorobenzoate have been widely investigated. The temperature range examined in these studies is relatively narrow (ca.  $20$ – $60$  °C) as the viscosity falls to a low value at high temperatures. At  $60$  °C, the relative viscosity  $\eta_r$  (given by  $\eta_0/\eta_s$  where  $\eta_s$  is the viscosity of the solvent, water) is usually below  $10^4$ . There are few, if any, examples of micellar solutions showing high viscosities ( $\eta_r > 10^4$ ) above  $60$  °C.

Here we examine two  $C_{22}$  surfactants with a cis unsaturation at the 13-carbon position: erucyl bis(hydroxyethyl)methylammonium chloride (EHAC) and erucyl trimethylammonium chloride (ETAC). The surfactants are studied in the presence of either sodium salicylate (NaSal) or sodium chloride (NaCl), which have binding or nonbinding counterions, respectively. Wormlike micelles formed by these surfactants show significantly enhanced viscoelasticity. The solutions exhibit very high viscosities ( $\eta_r \approx 10^7$ ) or gel-like behavior at room temperature, and they retain appreciable viscosity ( $\eta_r > 10^4$ ) for temperatures up to ca.  $90$  °C.

Previous studies of similar surfactants with long, mono-unsaturated tails mostly focused on their drag-reducing ability.<sup>17–21</sup> Surfactants with unsaturated tails effectively

\* To whom correspondence should be addressed. E-mail: kaler@che.udel.edu. Tel.: (302) 831-3553. FAX: (302) 831-1048.

- (1) Rehage, H.; Hoffmann, H. *Mol. Phys.* **1991**, *74*, 933.
- (2) Hoffmann, H. In *Structure and Flow in Surfactant Solutions*; ACS Symp. Ser. 578; Herb, C. A., Prudhomme, R., Eds.; American Chemical Society: Washington, DC, 1994; pp 2–31.
- (3) Cates, M. E. *Macromolecules* **1987**, *20*, 2289.
- (4) Granek, R.; Cates, M. E. *J. Chem. Phys.* **1992**, *96*, 4758.
- (5) Cates, M. E.; Candau, S. J. *J. Phys. Condens. Matter* **1990**, *2*, 6869.
- (6) Magid, L. J. *J. Phys. Chem.* **1998**, *102*, 4064.
- (7) Candau, S. J.; Hirsch, E.; Zana, R.; Delsanti, M. *Langmuir* **1989**, *5*, 1225.
- (8) Kern, F.; Zana, R.; Candau, S. J. *Langmuir* **1991**, *7*, 1344.
- (9) Fischer, P.; Rehage, H. *Langmuir* **1997**, *13*, 7012.
- (10) Makhlofi, R.; Cressely, R. *Colloid Polym. Sci.* **1992**, *270*, 1035.
- (11) Berret, J.-F.; Porte, G.; Decruppe, J.-P. *Phys. Rev. E* **1997**, *55*, 1668.
- (12) Ponton, A.; Schott, C.; Quemada, D. *Colloids Surf.* **1998**, *145*, 37.
- (13) Kern, F.; Lequeux, F.; Zana, R.; Candau, S. J. *Langmuir* **1994**, *10*, 1714.
- (14) Soltero, J. F. A.; Puig, J. E. *Langmuir* **1996**, *12*, 2654.

- (15) Hassan, P. A.; Candau, S. J.; Kern, F.; Manohar, C. *Langmuir* **1998**, *14*, 6025.
- (16) Oda, R.; Narayanan, J.; Hassan, P. A.; Manohar, C.; Salkar, R. A.; Kern, F.; Candau, S. J. *Langmuir* **1998**, *14*, 4364.
- (17) Manohar, C.; Kern, F.; Lequeux, F.; Candau, S. J. *Langmuir* **1997**, *13*, 5235.
- (18) Smith, B. C.; Chou, L. C.; Zakin, J. L. *J. Rheol.* **1994**, *38*, 73.
- (19) Rose, G. D.; Foster, K. L. *J. Non-Newtonian Fluid Mech.* **1989**, *31*, 59.
- (20) Rose, G. D.; Teot, A. S. In *Structure and Flow in Surfactant Solutions*; ACS Symp. Ser. 578; Herb, C. A., Prudhomme, R., Eds.; American Chemical Society: Washington, DC, 1994; pp 352–369.

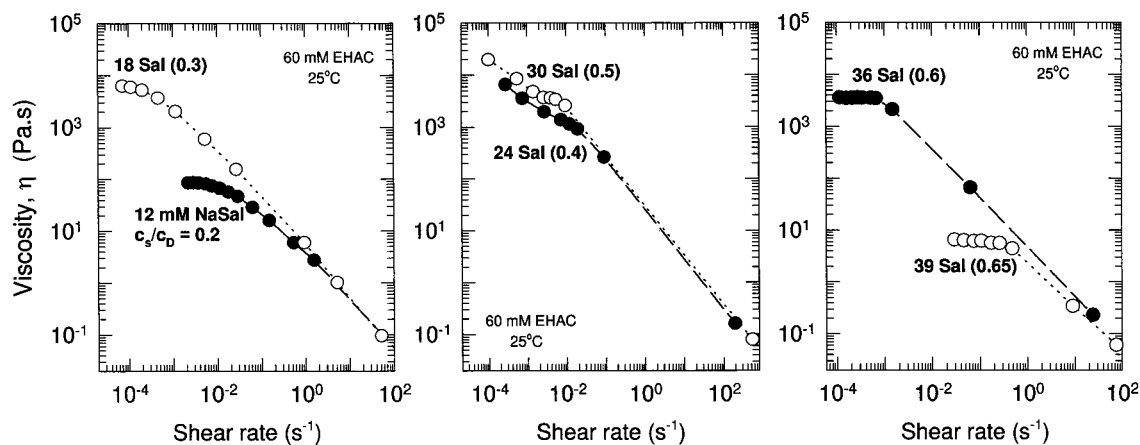


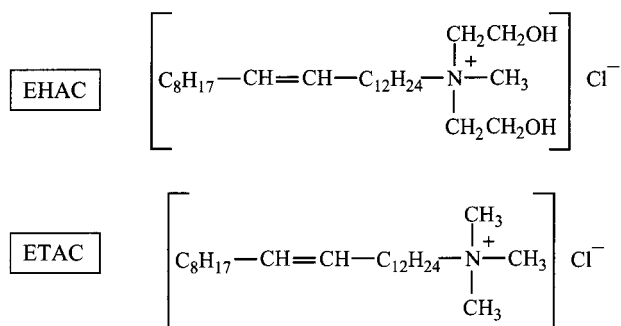
**Figure 1.** Effect of NaSal/EHAC molar ratio ( $c_s/c_D$ ) on the steady-shear rheology at 25 °C. The EHAC concentration is held constant at 60 mM.

reduced drag at higher temperatures than their saturated counterparts.<sup>18</sup> Some limited rheological data were reported in these studies, but only for low surfactant concentrations (<5 mM). The focus of this study is on much higher concentrations, well into the semidilute regime (above the overlap concentration  $c^*$ ).

Solutions of these  $C_{22}$  surfactants also show complex phase behavior in the presence of salt.<sup>22</sup> EHAC/NaCl solutions phase-separate at high salt content (ca. 2 M), while EHAC/NaSal solutions phase-separate beyond a certain molar ratio of salt to surfactant. These differences are linked to the fact that the  $\text{Cl}^-$  counterion does not penetrate the surfactant aggregate, while the hydrophobic salicylate counterions can insert between the charged headgroups, thus screening electrostatic repulsions and promoting micellar growth even at low salt concentrations.<sup>17</sup> The phase behavior is discussed in detail elsewhere;<sup>22</sup> all the solutions described here are single micellar phases.

### Experimental Section

**Materials.** EHAC and ETAC surfactants were commercial products from Akzo Nobel, Chicago, IL, and Witco Chemical Corp., Memphis, TN, respectively. Their chemical structures are shown below. Some polydispersity (10–15%) is expected in the hydrocarbon chain length, and only about 85% of the chains may be unsaturated. The surfactants were dried to constant weight in a vacuum oven at 40 °C. Sodium salicylate (*o*-hydroxy benzoate) and sodium chloride were ACS grade reagents purchased from



Aldrich. Solutions containing surfactant and salt were prepared using distilled–deionized water.

**Rheology.** Rheological experiments were performed on a Bohlin CS-10 stress-controlled rheometer. A couette geometry with a cup of 27.5 mm diameter and a bob of 25 mm diameter and 37.5 mm length was used. The cell was heated by a reservoir of fluid circulating from a Julabo high-temperature bath. A cover made of temperature-resistant silicone polymer was used to minimize sample evaporation. The sample was equilibrated for at least 20 min at each temperature prior to conducting experiments. Both steady and dynamic rheological experiments were performed at each temperature. The frequency spectra were conducted in the linear viscoelastic regime of the samples, as determined previously by dynamic stress sweep measurements. For the steady-shear experiments, an equilibration time of 90 s was given at each shear stress.

### Results

Rheological properties of EHAC/NaSal solutions are examined at 25 °C under steady shear (Figure 1) and dynamic shear (Figure 2). The solutions contain a fixed EHAC concentration  $c_D$  of 60 mM and varying concentrations of NaSal  $c_s$ , with the salt to surfactant molar ratio ( $c_s/c_D$ ) ranging from 0.2 to 0.65. For  $c_s/c_D = 0.2$ , the solution exhibits a zero-shear viscosity  $\eta_0$  around 100 Pa·s. Increasing the ratio to 0.3 results in a large increase in  $\eta_0$  to a value ca. 6000 Pa·s. Correspondingly, a much more elastic response is seen in dynamic shear. The relaxation time  $t_R$ , given by  $1/\omega_c$  where  $\omega_c$  is the frequency at which  $G'$  and  $G''$  crossover, is about 5 s at a ratio of 0.2. At ratios between 0.3 and 0.5, however,  $\omega_c$  is too low to measure, so the relaxation times are extremely long. Samples at  $c_s/c_D = 0.4$  and 0.5 also do not show a viscosity plateau at low shear-rates; instead the viscosity continues to rise with decreasing shear-rate. The low-shear viscosity plateau reappears for a ratio of 0.6 at a value around 3000 Pa·s. Increasing the ratio to 0.65 causes a dramatic drop in  $\eta_0$  by more than 2 orders of magnitude. Further increase in molar ratio beyond 0.65 results in phase separation.<sup>22</sup>

Samples at intermediate NaSal/EHAC ratios are gel-like, i.e., have characteristics of a solid with infinite relaxation time and viscosity. This unusual behavior is in contrast to the typical rheology of wormlike micellar solutions where a viscosity plateau is always found in the low-shear limit and a terminal region is always seen in frequency spectra.<sup>2</sup> For solutions with  $c_s/c_D = 0.4$  and 0.5, the viscosities at very low shear-rates are only apparent values since the solutions were equilibrated only for 90 s at each point in these tests. Creep experiments conducted at low shear-stresses indicate that the strain continues

(20) Lu, B.; Li, X.; Zakin, J. L.; Talmon, Y. *J. Non-Newtonian Fluid Mech.* **1997**, *71*, 59.

(21) Lu, B.; Zheng, Y.; Davis, H. T.; Scriven, L. E.; Talmon, Y.; Zakin, J. L. *Rheol. Acta* **1998**, *37*, 528.

(22) Raghavan, S. R.; Edlund, H.; Kaler, E. W. Manuscript in preparation.

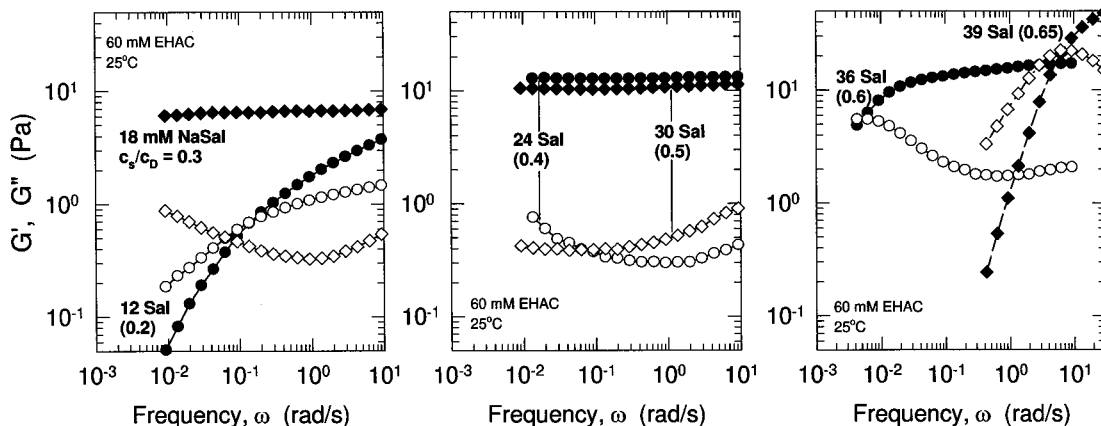


**Figure 2.** Effect of NaSal/EHAC molar ratio ( $c_s/c_D$ ) on the dynamic rheology at 25 °C. The elastic modulus  $G'$  (filled symbols) and viscous modulus  $G''$  (unfilled symbols) are plotted as a function of frequency. The EHAC concentration is held constant at 60 mM.

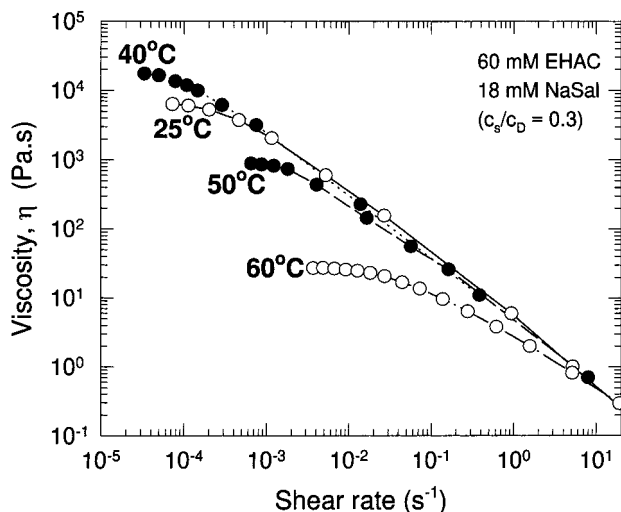


**Figure 3.** Effect of temperature on the viscosity of a sample containing 60 mM EHAC and 18 mM NaSal.

to increase slowly (but at a decreasing rate) over several hours, implying a continuous rise in viscosity toward infinite values. This suggests that the material has an apparent yield stress, and indeed the samples are able to support their own weight under gravity. The samples have

a transparent, gel-like appearance, and bubbles can be found trapped in them. The samples are also strongly flow birefringent—small stresses induced by a tilt or mild tapping of a sample vial are enough to cause intense birefringence when viewed under crossed polars. There is no birefringence at rest, however.

Unusual trends are also found in the rheology as a function of temperature. Instead of decreasing monotonically over the entire temperature range, the rheological properties show an initial enhancement at low temperatures followed by a subsequent decrease at higher temperatures. For a sample of 60 mM EHAC with NaSal at  $c_s/c_D = 0.3$ ,  $\eta_0$  increases by a factor of 2 from 25 to 40 °C (Figure 3), and concomitantly, the plateau modulus  $G_p$  increases by a similar amount (Figure 4). Beyond 40 °C,  $\eta_0$  decreases by more than 2 orders of magnitude over a 20 °C span. The frequency spectrum at 50 °C shows a crossover of  $G'$  and  $G''$  within the range of accessible frequencies. This crossover point shifts to higher frequencies as temperature is increased, indicating a decreasing relaxation time  $t_R$  in the high-temperature range.

The high-temperature rheology of a 60 mM EHAC solution at  $c_s/c_D = 0.5$  shows the Maxwellian character typical of wormlike micelles (Figure 5). At low temperatures (25–50 °C) (data not shown), the sample is gel-like and there is no low-shear viscosity plateau. The plateau

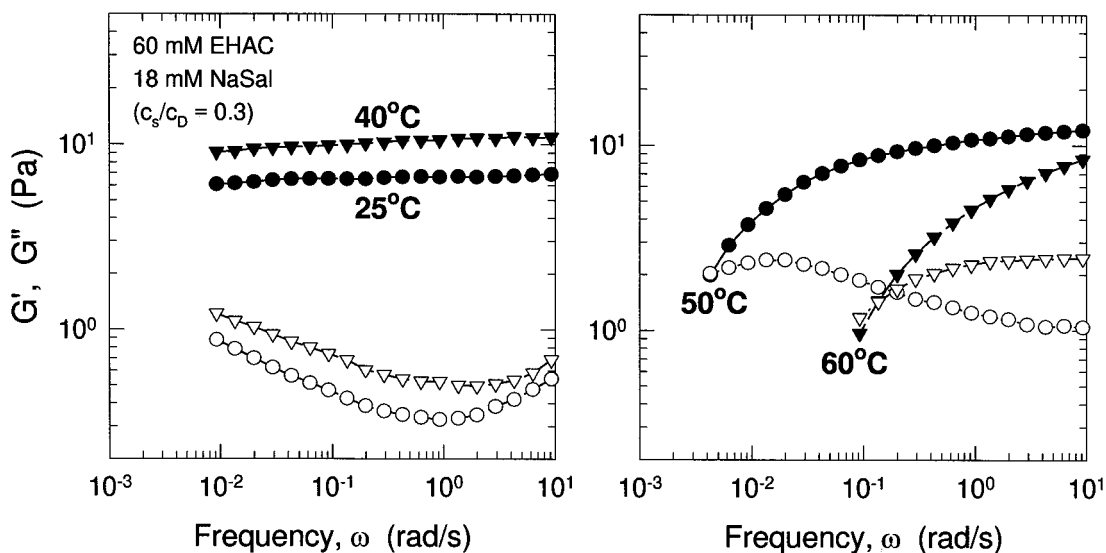


**Figure 4.** Effect of temperature on the elastic modulus  $G'$  (filled symbols) and viscous modulus  $G''$  (unfilled symbols) for a sample containing 60 mM EHAC and 18 mM NaSal.

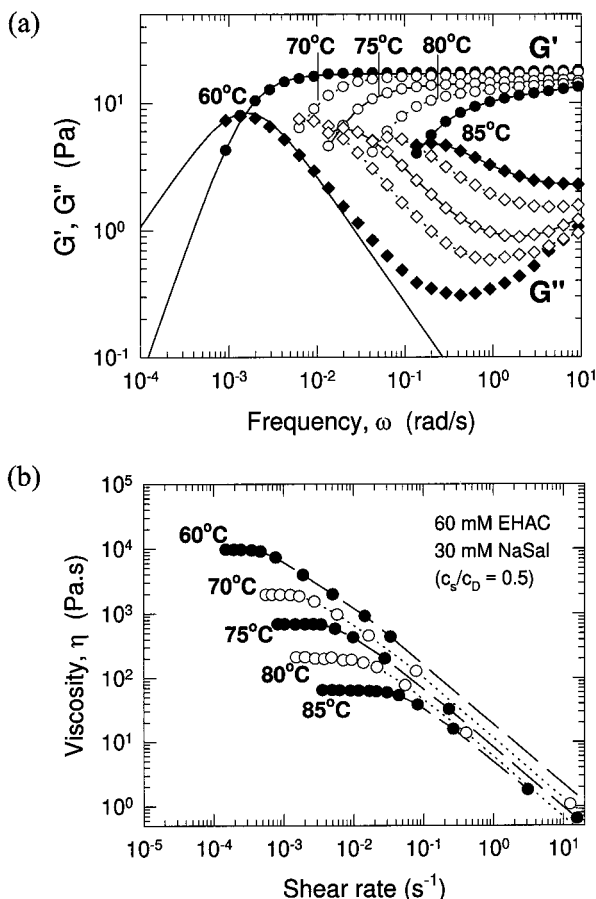


**Figure 5.** Effect of temperature on the rheology of a sample containing 60 mM EHAC and 30 mM NaSal: (a) dynamic frequency spectra; (b) steady-shear viscosity plots. The lines through the 60 °C data in (a) are fits to the Maxwell model.

modulus  $G_p$  shows a small increase in this temperature range. For temperatures of 60 °C and above, the rheology becomes characteristic of a Maxwell fluid with a single relaxation time. The dynamic moduli can then be described by:<sup>23</sup>

$$G'(\omega) = \frac{G_p \omega^2 t_R^2}{1 + \omega^2 t_R^2} \quad (1)$$

$$G''(\omega) = \frac{G_p \omega t_R}{1 + \omega^2 t_R^2} \quad (2)$$

The zero-shear viscosity of a Maxwell fluid is given by:<sup>23</sup>

$$\eta_0 = G_p t_R \quad (3)$$

The frequency spectrum (Figure 5a) shows fits of the  $G'$  and  $G''$  data at 60 °C to the Maxwell model. The model adequately describes the data except at high frequencies where an upturn in  $G''$  occurs due to the appearance of “breathing” or Rouse relaxation modes.<sup>4</sup> The viscosity data at 60 °C (Figure 5b) show a low-shear plateau, and the zero-shear viscosity  $\eta_0$  satisfies eq 3. Note that the  $\eta_0$  for this sample at 60 °C (ca.  $10^4$  Pa·s) exceeds the viscosity of most micellar solutions at room temperature. On increase of the temperature, the frequency spectrum is shifted in the direction of higher frequencies (shorter time

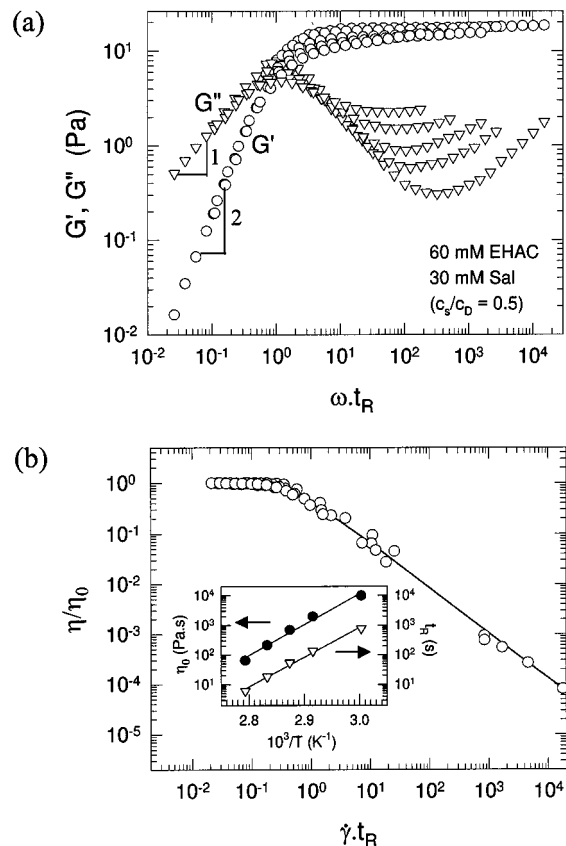


**Figure 6.** Rheological master curves for (a) dynamic shear and (b) steady shear for the 60 mM EHAC + 30 mM NaSal sample, obtained by scaling the data generated at various temperatures (Figure 5). The inset in (b) shows an Arrhenius plot of the zero-shear viscosity  $\eta_0$  and relaxation time  $t_R$  vs  $1/T$ . The slopes of the two straight lines here are identical and yield the activation energy  $E_a$ .

scales) while the plateau modulus  $G_p$  remains about the same. Correspondingly, the zero-shear viscosity  $\eta_0$  decreases steadily with temperature and attains a value ca. 65 Pa·s at 85 °C.

The qualitative similarity in the response at various temperatures enables the above data to be scaled onto master curves.<sup>9–12</sup> For the dynamic rheological data, this is done by plotting the moduli ( $G'$ ,  $G''$ ) against frequency scaled by the relaxation time  $t_R$  at the corresponding temperature (Figure 6a). The data at low frequencies collapses onto a single pair of  $G'$  and  $G''$  curves with slopes of 2 and 1, respectively. Due to the appearance of “breathing” modes at high frequencies, the  $G''$  curves do not overlap in this range.<sup>9</sup> A master plot of the steady-shear data requires scale factors for each axis (Figure 6b). The ordinate is a reduced viscosity, i.e.,  $\eta$  divided by the zero-shear viscosity  $\eta_0$  at the corresponding temperature, while the shear-rate axis is scaled by the relaxation time  $t_R$  from dynamic rheology, as was done in Figure 6a. This scaling nicely collapses the viscosity data.

The variation of  $\eta_0$  and  $t_R$  with temperature can be empirically described by Arrhenius relationships, indicating exponential reductions in these quantities:<sup>7,9</sup>

$$t_R = A e^{E_a/RT} \quad (4)$$

$$\eta_0 = G_p A e^{E_a/RT} \quad (5)$$

Here  $E_a$  is the flow activation energy,  $R$  is the gas constant, and  $A$  is a pre-exponential factor. Semilogarithmic plots

(23) Larson, R. G. *The Structure and Rheology of Complex Fluids*; Oxford University Press: Oxford, 1999.

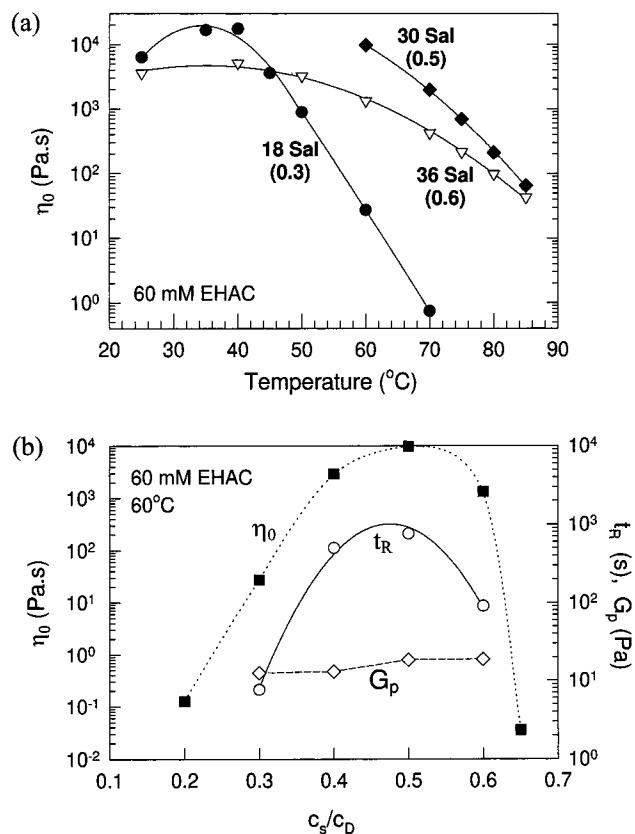


**Figure 7.** (a) Effect of temperature on the zero-shear viscosity  $\eta_0$  for different molar ratios of NaSal to EHAC ( $c_s/c_D$ ). (b) Effect of NaSal to EHAC molar ratio on the rheological parameters at a constant temperature of 60 °C. The EHAC concentration is held constant at 60 mM in all cases.

of  $\eta_0$  and  $t_R$  vs  $1/T$  (Figure 6b, inset) fall on straight lines with identical slopes, consistent with eqs 4 and 5 since  $G_p$  is independent of temperature. The calculated value of  $E_a$  is 198 kJ/mol or about  $80 kT$ . This falls in the range of  $E_a$  values found for other wormlike micellar solutions.<sup>7-9,13-15</sup>

Figure 7a shows the variation of zero-shear viscosity  $\eta_0$  with temperature for three different molar ratios of NaSal/EHAC. Samples with  $c_s/c_D = 0.3$  and  $0.6$  both exhibit a modest viscosity maximum at low temperatures followed by a steady drop in  $\eta_0$  at higher temperatures. Viscosity data are not shown at low temperatures for the  $c_s/c_D = 0.5$  sample due to lack of a well-defined low-shear viscosity plateau. The decay in viscosity with temperature is rapid at low NaSal content ( $c_s/c_D = 0.3$ ) and more gradual at higher NaSal content ( $c_s/c_D = 0.6$ ). For each sample, the Arrhenius relationship for the viscosity is obeyed only in the high-temperature limit.

Rheological parameters ( $\eta_0$ ,  $t_R$ ,  $G_p$ ) are examined as a function of NaSal/EHAC molar ratio at a constant temperature of 60 °C (Figure 7b). The plateau modulus  $G_p$  stays approximately constant with varying NaSal content. On the other hand, both  $\eta_0$  and  $t_R$  describe pronounced maxima around  $c_s/c_D = 0.5$ . (Only  $\eta_0$  is shown at ratios of 0.2 and 0.65 because these two samples were too thin at 60 °C to perform dynamic rheology.) Note that  $\eta_0$  increases by 5 orders of magnitude to its maximum value and, with further increase in NaSal content, decreases by 5 orders of magnitude.

The effect of surfactant concentration  $c_D$  is studied at a fixed NaSal/EHAC molar ratio  $c_s/c_D = 0.5$  which represents the optimal ratio from Figure 7. Rheological parameters are again examined at a constant temperature of 60 °C as a function of  $c_D$  (Figure 8). The plateau modulus

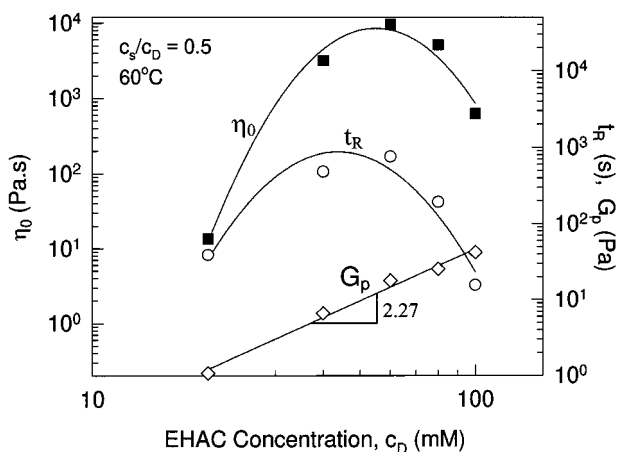


**Figure 8.** Effect of EHAC concentration on the rheological parameters at a constant temperature of 60 °C. The NaSal/EHAC molar ratio  $c_s/c_D$  is held constant at 0.5.

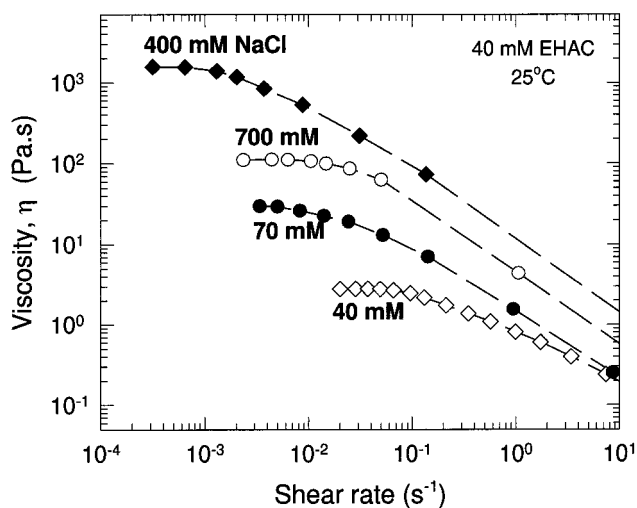


**Figure 9.** Effect of NaCl concentration on the viscosity of 40 mM EHAC solutions at 25 °C.

$G_p$  exhibits a power law,  $G_p \sim c_D^{2.27}$ , which is close to the theoretical prediction for polymers and wormlike micelles in solution.<sup>3,5</sup> However, both  $\eta_0$  and  $t_R$  again describe maxima at intermediate concentrations, with the  $\eta_0$  maximum occurring around  $c_D = 60$  mM. Thus the composition for optimal rheology consists of 60 mM EHAC surfactant and 30 mM NaSal, which correspond on a weight basis to ca. 2.7 wt % surfactant and 0.5 wt % salt.

The effect of a nonbinding salt (NaCl) is studied at 25 °C for a fixed EHAC concentration of 40 mM (Figure 9). The viscosity  $\eta_0$  remains quite low at low NaCl content and reaches significantly high values ( $\approx 10^3$  Pa·s) only around 100 mM NaCl. As with NaSal, there is a drop in  $\eta_0$  at higher NaCl concentrations. Note that much higher concentrations of NaCl are required to produce high viscosities compared to NaSal. This is because while salicylate counterions can penetrate between the headgroups into the hydrophobic interior of micelles, the  $Cl^-$  counterion cannot do so.<sup>17</sup> Thus higher concentrations of  $Cl^-$  are necessary for screening the repulsions between headgroups.

Finally, the effect of headgroup structure is studied by comparing EHAC and ETAC surfactants which have identical tails and bis(hydroxyethyl)methylammonium and trimethylammonium headgroups, respectively. The rheology is compared for a surfactant concentration of 60 mM and a salt (NaSal) concentration of 30 mM, corre-

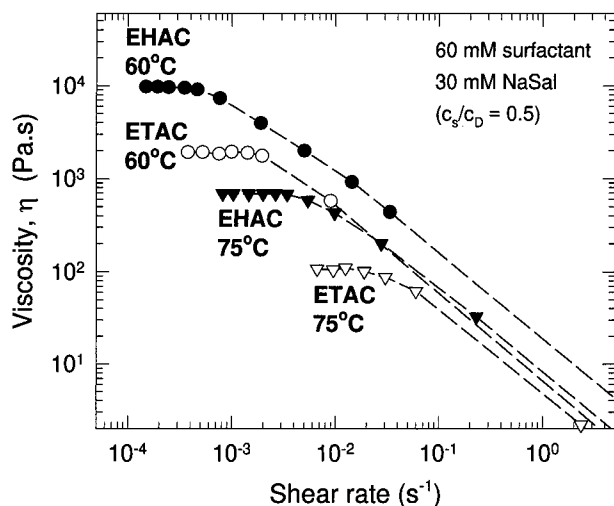


**Figure 10.** Effect of headgroup structure on the viscosity. Two surfactants with identical tails and different headgroups are compared: ETAC (trimethylammonium) and EHAC (bis-(hydroxyethyl)methylammonium). Data are shown at 60 and 75 °C for solutions containing 60 mM surfactant and 30 mM NaSal.

sponding to  $c_s/c_D = 0.5$  (Figure 10). The ETAC sample shows a zero-shear viscosity which is an order-of-magnitude lower than that of the EHAC sample at both 60 and 75 °C. Both samples show gel-like rheology at lower temperatures, with identical values of their plateau moduli (data not shown). The headgroup in EHAC features a positively charged nitrogen atom shielded by bulky, polar moieties, so electrostatic repulsions between these headgroups may be low relative to ETAC. Lower repulsions would favor micellar growth, which would explain the higher viscosities for EHAC.

### Discussion

The samples studied here are highly viscoelastic or even gel-like. Gel-like behavior has been seen with other surfactant phases such as close-packed vesicles or cubic phases.<sup>24</sup> Wormlike micellar systems, on the other hand, are not true gels since they only form entanglement networks and always show a terminal region in their frequency spectra. The lack of a terminal region and the existence of a yield stress for some of our samples are not necessarily consistent with micellar systems. However, the Maxwellian frequency spectra at high temperatures (Figure 5a) are a distinctive characteristic of wormlike micellar fluids. Moreover, the fact that all samples are clear, isotropic solutions at rest and strongly birefringent under flow (features which are present at all temperatures) also points to wormlike micelles. Data from small-angle neutron scattering (SANS) on these solutions is also consistent with the presence of wormlike micelles.<sup>22</sup>

The enhancement in rheology at low temperatures is primarily reflected in the plateau modulus  $G_p$  which increases from 25 to 40 °C and then remains constant (Figure 4). Since  $G_p$  correlates with the number density of wormlike chains incorporated into the entanglement network, the initial increase in  $G_p$  suggests that not all of the surfactant forms wormlike micelles at low temperatures or that not all micelles are long enough to entangle. Apparently, only at high temperatures is the surfactant completely incorporated into entangling micellar chains. This effect cannot be due to incomplete

surfactant dissolution since the samples are well above the Krafft temperature, and moreover, the solutions are optically clear and isotropic over the entire temperature range. A viscosity maximum as a function of temperature is also shown by solutions of a hybrid hydrocarbon-fluorocarbon surfactant.<sup>25</sup>

The strong rheological response at low temperatures translates to appreciable solution viscosities even at high temperatures. For example, the sample in Figure 5 shows a zero-shear viscosity  $\eta_0$  of 65 Pa·s at 85 °C (i.e., a relative viscosity  $\eta_r \approx 10^5$ ). Such a high viscosity has never before been reported for micellar solutions at comparable temperatures. For most micellar systems,  $\eta_0$  is reduced below 10 Pa·s by about 60 °C. Extrapolating the viscosity data in Figure 5b to higher temperatures,  $\eta_0$  falls to 10 Pa·s around 93 °C and to 2 Pa·s around 100 °C. Thus, even at 100 °C,  $\eta_r \approx 7000$ ; i.e., the viscosity of the sample is 7000 times that of water at that temperature, representing a significant viscosity enhancement.

The question then is why the EHAC surfactant offers such an extreme rheological response. The distinguishing features of EHAC are the long, unsaturated chain and the complex headgroup. Changing the headgroup (EHAC to ETAC) is not found to alter the essential features in the rheology, so the hydrophobic tail is of primary importance. Because the tail features a cis-double bond, the surfactant is difficult to crystallize and its Krafft point is very low (<0 °C).<sup>18</sup> The hydrophilic headgroup in EHAC also aids dissolution in water. EHAC thus dissolves easily whereas a saturated-chain surfactant such as octadecyl trimethylammonium bromide ( $C_{18}$ TAB) is insoluble in water under ambient conditions. The long ( $C_{22}$ ) hydrophobic tails also give low critical micelle concentrations, and by extension, the cylindrical micelles formed in the presence of salt should have a low overlap concentration  $c^*$ . The large hydrophobes may also contribute to a high end-cap energy  $E_c$  (the energy required to create two end caps by breaking a micelle), thus favoring the growth of longer micelles.

The micellar contour length  $\bar{L}$  can be quantified via the expression of Granek and Cates<sup>4</sup> in terms of the value of  $G'_{\min}$  at its minimum:

$$\frac{G'_{\min}}{G_p} \approx \frac{l_e}{\bar{L}} \quad (6)$$

The contour length  $\bar{L}$  can thus be estimated from rheology if the entanglement length  $l_e$  is known.  $l_e$  is the average contour length between two entanglement points and is related to the persistence length  $l_p$  of the micelles and the network mesh size  $\xi$ .<sup>5,6</sup> The mesh size can be readily obtained from the plateau modulus  $G_p$ . The persistence length  $l_p$  is the length scale over which the micelles act as rigid entities (typically  $\bar{L} \gg l_p$ ). No reliable estimates of  $l_p$  are currently available for EHAC micelles. However, eq 6 indicates that for a given  $l_e$ ,  $\bar{L}$  is inversely related to the ratio  $G'_{\min}/G_p$ . The  $G'_{\min}/G_p$  value at 60 °C for the EHAC/NaSal sample in Figure 5a is about 0.016. Comparisons with literature suggest that this is the lowest value yet reported for wormlike micelles.<sup>6,13,14,27,28</sup> The lowest reported value thus far for  $G'_{\min}/G_p$  is 0.024 for micelles of cetyl trimethylammonium dichlorobenzoate at 25 °C.<sup>26</sup> This implies that EHAC micelles at 60 °C are comparable in length or longer than other micelles at room temperature. Typical values of  $l_e$  in other systems range

(25) Tobita, K.; Sakai, H.; Kondo, Y.; Yoshino, N.; Kamogawa, K.; Momozawa, N.; Abe, M. *Langmuir* **1998**, *14*, 4753.

(26) Carver, M.; Smith, T. L.; Gee, J. C.; Delichere, A.; Caponetti, E.; Magid, L. J. *Langmuir* **1996**, *12*, 691.

(24) Hoffmann, H.; Ulbricht, W. *Curr. Opin. Colloid Interface Sci.* **1996**, *1*, 726.

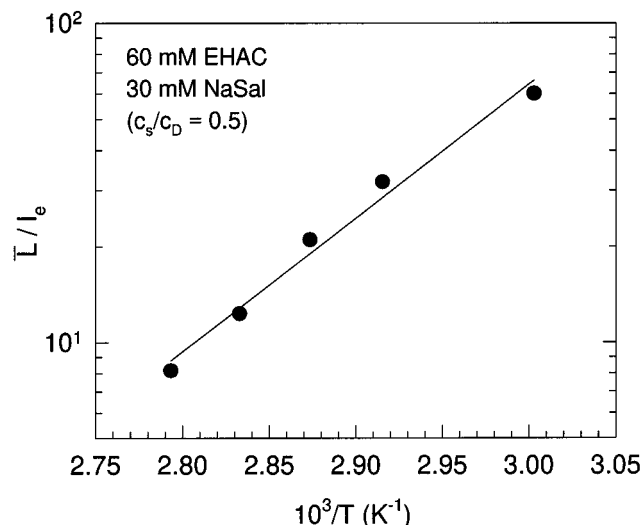


**Figure 11.** Ratio of overall contour length  $\bar{L}$  to entanglement length  $l_e$  for wormlike micelles in the 60 mM EHAC + 30 mM NaSal sample plotted vs  $1/T$  in an Arrhenius plot. The slope yields the end-cap energy  $E_c$  of the micelles.

between 80 and 150 nm,<sup>6,26</sup> which would yield a contour length  $\bar{L}$  of 5–10  $\mu\text{m}$  for EHAC micelles.

As temperature increases, the value of  $G''$  at its minimum point also increases (Figure 5a) while the plateau modulus  $G_p$  stays constant. This means that  $G''_{\text{min}}/G_p$  increases, or equivalently, by eq 6,  $\bar{L}/l_e$  decreases with temperature. Because  $G_p$  is relatively independent of temperature, the mesh size  $\xi$  and hence the entanglement length  $l_e$  are also independent of temperature.<sup>9</sup> The decrease in  $\bar{L}/l_e$  therefore implies a decrease in contour length  $\bar{L}$  with temperature, as is expected for wormlike micelles. To quantify this effect, we use the mean-field result for the variation in  $\bar{L}$  with surfactant volume fraction  $\phi$  and temperature:<sup>5</sup>

$$\bar{L} \sim \phi^{1/2} \exp[E_c/2kT] \quad (7)$$

The parameter that controls the reduction in micellar length with temperature is the end-cap energy  $E_c$ . Because  $l_e$  is independent of temperature, a semilogarithmic plot of  $G_p/G''_{\text{min}} \equiv \bar{L}/l_e$  vs  $1/T$  allows  $E_c$  to be estimated from the slope. (Thus, precise values of  $\bar{L}$  are not required to obtain  $E_c$ .) Figure 11 shows such a plot constructed from the data in Figure 5a. The Arrhenius relationship for  $\bar{L}$  is confirmed, and the slope yields a value for  $E_c$  of 160 kJ/mol or 65  $kT$ . This is rather high compared to the  $E_c$  values reported for  $C_{16}$  surfactant micelles (ca. 20  $kT$ )<sup>7,14</sup> and comparable to the  $E_c$  obtained for micelles of a dimeric (gemini) surfactant (40–70  $kT$ ).<sup>13</sup> Note that eq 7 is strictly valid only for electrostatically screened micelles. When electrostatic repulsions persist between the surface charges, the net scission energy of a micelle is reduced relative to  $E_c$ .<sup>13</sup> The  $E_c$  value obtained here pertains to a low NaSal concentration that is probably insufficient for

complete screening; therefore, this value of  $E_c$  must be considered a lower estimate.

The molecular structure of the surfactant thus contributes to a high  $E_c$ , i.e., to a high energy cost for micellar scission. This tilts the thermodynamic balance in favor of micellar growth, resulting in extremely long wormlike micelles. An entangled network of such micelles can account for the strong viscoelasticity of the system. The gel-like behavior at low temperatures may simply be the consequence of these long chains taking an abnormally long time to relax by reptation (the time scale for reptation increases rapidly with micellar contour length:  $\tau_{\text{rep}} \sim \bar{L}^3$ ).<sup>5</sup> This argument implies that the samples are not “true gels” but show a finite relaxation time which may however fall well outside the window of accessible time scales. Further studies are required to clarify this issue.

Viscosity maxima as a function of salt and surfactant concentration are ubiquitous in the literature.<sup>2,6</sup> Several cationic surfactants have been studied in conjunction with NaSal, and in each case a viscosity maximum occurs as a function of salt content.<sup>27–29</sup> For the cetyl trimethylammonium chloride ( $C_{16}\text{TAC}$ ) + NaSal system, the maximum occurs at  $c_s/c_D = 0.6$ ,<sup>27</sup> in near agreement with the results for EHAC + NaSal. Viscosity maxima are also observed as a function of surfactant concentration at a constant ratio of salt to surfactant, including in the  $C_{16}\text{TAC}$  + NaSal system.<sup>8,29</sup> The reasons for these maxima are not yet clearly understood, but the possibilities include a transition from linear to branched micelles or a maximum in micellar contour length.<sup>6,13</sup>

## 5. Conclusions

The cationic surfactant EHAC in water gives rise to highly viscoelastic or gel-like solutions on addition of salt, and these solutions retain appreciable viscosities up to high temperatures (above 90 °C). The surfactant is thus an attractive candidate for rheology-control applications. The rheological behavior can be rationalized in terms of an entangled network of extremely long wormlike micellar chains. Due to their enormous length, the chains may take an unusually long time to relax by reptation. The enhanced micellar growth may be facilitated by an abnormally high end-cap energy  $E_c$  which in turn may be linked to the long, unsaturated surfactant tails. Small concentrations of a binding counterion (NaSal) are enough to produce viscoelastic solutions, and the rheology shows a pronounced maximum as a function of the NaSal/EHAC molar ratio. Higher concentrations of a nonbinding salt (NaCl) are required for effecting high viscosities. Non-monotonic trends in viscosity are observed as a function of surfactant concentration and also as a function of temperature.

LA0007933

(27) Clausen, T. M.; Vinson, P. K.; Minter, J. R.; Davis, H. T.; Talmon, Y.; Miller, W. G. *J. Phys. Chem.* **1992**, *96*, 474.

(28) Aswal, V. K.; Goyal, P. S.; Thiyagarajan, P. *J. Phys. Chem. B* **1998**, *102*, 2469.

(29) Ait Ali, A.; Makhlofi, R. *Phys. Rev. E* **1997**, *56*, 4474.